Macrophage LC3-associated phagocytosis is an immune defense against *Streptococcus pneumoniae* that diminishes with host aging

Megumi Inomata[a,b], Shuying Xu[a,c], Pallavi Chandra[d,e], Simin N. Meydani[f], Genzou Takemura[g], Jennifer A. Philips[d,e], and John M. Leong[a,1]

[a]Department of Molecular Biology and Microbiology, Tufts University School of Medicine, Boston, MA 02111; [b]Department of Oral Microbiology, Asahi University School of Dentistry, Mizuho, 501-0296 Gifu, Japan; [c]Graduate Program in Immunology, Tufts Graduate School of Biomedical Sciences, Boston, MA 02111; [d]Department of Medicine, Division of Infectious Diseases, Washington University School of Medicine, St. Louis, MO 63110; [e]Department of Molecular Microbiology, Washington University School of Medicine, St. Louis, MO 63110; [f]Jean Mayer USDA Human Nutrition Research Center on Aging at Tufts University, Boston, MA 02111; and [g]Department of Internal Medicine, Asahi University School of Dentistry, Mizuho, 501-0296 Gifu, Japan

Edited by Craig R. Roy, Yale University School of Medicine, New Haven, CT, and accepted by Editorial Board Member Carl F. Nathan November 17, 2020 (received for review July 22, 2020)

Streptococcus pneumoniae **is a leading cause of pneumonia and invasive disease, particularly, in the elderly. *S. pneumoniae* lung infection of aged mice is associated with high bacterial burdens and detrimental inflammatory responses. Macrophages can clear microorganisms and modulate inflammation through two distinct lysosomal trafficking pathways that involve 1A/1B-light chain 3 (LC3)-marked organelles, canonical autophagy, and LC3-associated phagocytosis (LAP). The *S. pneumoniae* pore-forming toxin pneumolysin (PLY) triggers an autophagic response in nonphagocytic cells, but the role of LAP in macrophage defense against *S. pneumoniae* or in age-related susceptibility to infection is unexplored. We found that infection of murine bone-marrow-derived macrophages (BMDMs) by PLY-producing *S. pneumoniae* triggered Atg5- and Atg7-dependent recruitment of LC3 to *S. pneumoniae*-containing vesicles. The association of LC3 with *S. pneumoniae*-containing phagosomes required components specific for LAP, such as Rubicon and the NADPH oxidase, but not factors, such as Ulk1, FIP200, or Atg14, required specifically for canonical autophagy. In addition, *S. pneumoniae* was sequestered within single-membrane compartments indicative of LAP. Importantly, compared to BMDMs from young (2-mo-old) mice, BMDMs from aged (20- to 22-mo-old) mice infected with *S. pneumoniae* were not only deficient in LAP and bacterial killing, but also produced higher levels of proinflammatory cytokines. Inhibition of LAP enhanced *S. pneumoniae* survival and cytokine responses in BMDMs from young but not aged mice. Thus, LAP is an important innate immune defense employed by BMDMs to control *S. pneumoniae* infection and concomitant inflammation, one that diminishes with age and may contribute to age-related susceptibility to this important pathogen.**

LC3-associated phagocytosis | bone-marrow-derived macrophages | *Streptococcus pneumoniae* | aging | autophagy

Streptococcus pneumoniae (pneumococcus) commonly colonizes the nasopharynx asymptomatically but is also capable of infecting the lower respiratory tract to cause pneumonia and spreading to the bloodstream to cause septicemia and meningitis (1). Susceptibility to pneumonia and invasive disease caused by *S. pneumoniae* is remarkably higher in individuals aged 65 and over, leading to high rates of mortality and morbidity in the elderly population (1, 2). In countries, such as the United States and Japan, deaths due to pneumococcal pneumonia have been on the rise in parallel with the rapid growth in the elderly population (3, 4).

A hallmark of pneumococcal pneumonia is a rapid and exuberant response by immune cells, such as neutrophils and macrophages. This innate immune response to *S. pneumoniae* lung infection is critical for pathogen clearance and the control of disease (5–7). Deficiencies in the number or function of innate phagocytic cells, such as neutropenia (8) or macrophage phagocytic receptor defects (9–12), lead to diminished pneumococcal clearance and increased risk of invasive pneumococcal disease in both mouse models and humans. Phagocytic activity in alveolar macrophages is important during early responses to subclinical infections (13–15), and during moderate *S. pneumoniae* lung infection, newly generated monocytes eggress from the bone marrow and migrate into the lungs, differentiating into monocyte-derived alveolar macrophages (16). In addition to directly eliminating the invading microbe, macrophages secrete key cytokines, such as tumor necrosis factor (TNF), interleukin-1β (IL-1β), and interleukin-6 (IL-6), that regulate effector cell functions and pulmonary inflammation (17–19).

Although an innate immune response is critical for pathogen clearance, poorly controlled inflammation can lead to tissue damage and mortality (20, 21). For example, in murine models, neutrophilic infiltration can enhance pulmonary damage and disrupt epithelial barrier function, leading to bacteremia and mortality (22–25). Macrophages are critical not only in regulating the early inflammatory response, but are also crucial for curtailing inflammation during the resolution phase of infection to limit tissue damage and promote healing (26, 27).

Significance

The elderly exhibit susceptibility to many infectious agents, including *S. pneumoniae*. A robust acute inflammatory response to *S. pneumoniae* is associated with severe disease. *S. pneumoniae* triggers canonical autophagy in nonprofessional phagocytes, but its role in macrophages is largely unexplored. We found that BMDMs utilize LAP, rather than canonical autophagy, to both eliminate *S. pneumoniae* and modulate inflammation. Notably, compared to young BMDMs, aged BMDMs were deficient in LAP, resulting in compromised bacterial killing and enhanced proinflammatory responses. Thus, *S. pneumoniae* triggers LAP in BMDMs, a process that controls both microbial numbers and tissue-damaging inflammation. Importantly, LAP diminishes with age and may contribute to the observed susceptibility of the elderly to many infectious diseases.

Author contributions: M.I., P.C., J.A.P., and J.M.L. designed research; M.I. and G.T. performed research; P.C., S.N.M., and J.A.P. contributed new reagents/analytic tools; M.I., G.T., J.A.P., and J.M.L. analyzed data; and M.I., S.X., J.A.P., and J.M.L. wrote the paper.

The authors declare no competing interest.

This article is a PNAS Direct Submission. C.R.R. is a guest editor invited by the Editorial Board.

[1]To whom correspondence may be addressed. Email: john.leong@tufts.edu.

This article contains supporting information online at https://www.pnas.org/lookup/suppl/doi:10.1073/pnas.2015368117/-/DCSupplemental.

First published December 21, 2020.

Elderly individuals have higher baseline and induced levels of inflammation, a phenomenon termed inflammaging (28), that contributes to many age-associated pathological conditions, including increased susceptibility to a variety of infectious diseases, such as *S. pneumoniae* infection (7, 28–30). *S. pneumoniae*-induced inflammation, characterized by increased levels of chemokines, proinflammatory cytokines, and decreased anti-inflammatory cytokines, such as IL-10, is enhanced in the elderly (29, 31) as well as in aged mice (32, 33) and correlates with ineffective immune responses. Age-related chronic exposure to TNF-α, for instance, dampens macrophage-mediated *S. pneumoniae* clearance during lung infection (34), and NLR family pyrin domain containing 3 inflammasome activation in macrophages diminishes upon aging in mice (35). However, the age-related changes in macrophage effector functions leading to diminished clearance of *S. pneumoniae* are incompletely understood.

One important means of macrophage-mediated pathogen clearance is1A/1B-light chain-3 (LC3)-associated phagocytosis (LAP), a process by which cells target phagocytosed extracellular particles for efficient degradation (36–38). LAP combines the molecular machineries of phagocytosis and autophagy, resulting in the conjugation of the autophagic marker, the microtubule-associated protein LC3, to phosphatidylethanolamine on the phagosomal membrane, generating so-called "LAPosomes" that undergo facilitated fusion with lysosomes (38, 39). Canonical autophagy targets cytoplasmic components, such as damaged subcellular organelles and intracellular microbes for sequestration into double-membrane autophagic vesicles (40, 41). In contrast, LAPosomes retain the single-membrane nature of phagosomes, and their formation requires overlapping but nonidentical genes compared to canonical autophagy (42). In addition to enabling efficient degradation of phagocytosed bacteria, LAP also plays important immune regulatory roles, such as in curtailing proinflammatory cytokine production during the subsequent innate immune response (39, 43). Indeed, the LAP-mediated microbial defense and immunomodulatory functions work together to limit tissue damage and restore homeostasis (38).

S. pneumoniae triggers canonical autophagy in epithelial cells and fibroblasts, and bacteria can be found in double-membrane vacuoles whose formation is dependent on autophagic machinery (44). Many bacterial pathogens that induce autophagy produce pore-forming toxins, which can damage endosomal membranes, thus, recruiting autophagic machinery to engulf injured organelles (45). Pneumococcus-induced autophagy is dependent on the cholesterol-dependent pore-forming toxin pneumolysin (PLY), which triggers the autophagic delivery of *S. pneumoniae* to lysosomes and results in bacterial killing (44, 46). Recently, a kinetic examination of *S. pneumoniae*-targeting autophagy in fibroblasts demonstrated that canonical autophagy was preceded by early and rapid PLY-dependent LAP (47). However, the requirements for this process were somewhat different from LAP in macrophages, and the pneumococcus-containing LAPosomes did not promote bacterial clearance but required subsequent transition to canonical autophagy to reduce bacterial numbers (46, 47).

In the current study, we found that *S. pneumoniae* infection of murine bone-marrow-derived macrophages (BMDMs) induces LAP in a PLY-dependent manners and that age-related defects in BMDM LAP contributed to diminished bactericidal activity and enhanced proinflammatory cytokine production. Our results suggest that PLY-induced LAP promotes bacterial clearance, and age-associated dysregulation of this process may contribute to enhanced bacterial survival, poorly regulated inflammation, and increased susceptibility to invasive pneumococcal disease.

Results

***S. pneumoniae* Triggers PLY-Dependent Lipidation of LC3, Which Is Recruited to Internalized Bacteria.** To determine if the autophagic process identified in nonimmune cells also occurs in macrophages, we infected murine BMDMs with *S. pneumoniae*. We found that infection of BMDM rapidly induced conversion of LC3-I to its vesicle-bound form LC3-II, indicating onset of autophagy or an autophagy-related process (Fig. 1*A*). To identify if specific bacterial components of *S. pneumoniae*, such as the cholesterol-dependent pore-forming cytolysin PLY, were required to trigger LC3 lipidation, we infected BMDMs with several *S. pneumoniae* mutants, including strains lacking pneumococcal surface protein A (Δ*pspA*), pneumococcal surface protein C (Δ*pspC*), capsule (Δ*cps*), or PLY (Δ*ply*). We found that the PLY-deficient strain failed to trigger LC3-I conversion to LC3-II (Fig. 1*A*).

To examine PLY-mediated autophagic processes in an experimental model that permits gene silencing approaches, we utilized murine RAW264.7 macrophages (48). As predicted, serum starvation, a documented inducer of autophagy (49), resulted in production of LC3-II (Fig. 1*B*). *S. pneumoniae* infection also triggered LC3-II production in these macrophages in a manner dependent on the multiplicity of infection (MOI) (Fig. 1*B*). Fluorescent microscopic examination of *S. pneumoniae*-infected cells that stably express a green fluorescent protein (GFP)-tagged LC3 protein (GFP-LC3) revealed that LC3 colocalized with ∼35% of intracellular *S. pneumoniae* within the first 0.5 h with colocalization gradually diminishing after 1 h (Fig. 1 *C* and *D*). PLY-deficient mutants of *S. pneumoniae* strains TIGR4 or D39 were significantly diminished for LC3 colocalization compared to wild-type (WT), and marker rescue of *S. pneumoniae* strain D39Δ*ply* reversed this defect (Fig. 1*E*). The endopeptidase PepO has been implicated in stimulation of peritoneal derived macrophage autophagy by *S. pneumoniae* strain D39 (50), but the inability of a PLY-deficient strain D39 to trigger LC3 colocalization indicates that PepO is insufficient to initiate the autophagic process. For the experiments described below, we utilized strain TIGR4. As expected, gene silencing of *Atg5* and *Atg7*, which encode proteins required for canonical autophagy and LAP, abolished both rapamycin (Rapa)-induced autophagic responses (*SI Appendix*, Fig. S1 *A* and *B*) as well as LC3 colocalization with *S. pneumoniae* (Fig. 1 *F* and *G* and *SI Appendix*, Fig. S1 *C* and *D*) as did chemical inhibition with the PI3K inhibitor 3-methyladenine (3-MA) (Fig. 1*H* and *SI Appendix*, Fig. S1*E*). Similarly, BMDMs lacking *Atg7* exhibited reduced recruitment of GFP-LC3 to *S. pneumoniae,* demonstrating that the requirement for ATG7 for LC3 colocalization with *S. pneumoniae* in primary cells (Fig. 1*I* and *SI Appendix*, Fig. S1*F*). Thus, *S. pneumoniae* infection triggers a PLY-dependent LC3 recruitment to internalized bacteria in BMDMs, an autophagic process that requires ATG5, ATG7, and PI3K.

***S. pneumoniae* Triggers LAP and Not Canonical Autophagy in Murine BMDMs.** LC3 conversion and recruitment to intracellular compartments occurs in both canonical autophagy and nonclassical processes, such as LAP. LC3 recruitment in canonical autophagy depends upon initiation and elongation of the phagophore and can take up to several hours to accomplish, whereas in LAP, recruitment has been observed as early as 15 min after infection and can wane after 1 h (40, 41). In our case, we observed a dramatic increase in LC3 recruitment to *S. pneumoniae* vesicles by 0.5-h postinfection that decreased after 1 h (Fig. 1 *C* and *D*), which led us to postulate that LAP rather than canonical autophagy drives LC3 recruitment to *S. pneumoniae*. To test our hypothesis, we initially examined the involvement of reactive oxygen species (ROS) production machinery in *S. pneumoniae* triggered LC3 recruitment as PLY induces the production of intracellular ROS in human neutrophils (51), and generation of ROS by the NADPH oxidase is often required for LAP (42, 52). We found that *S. pneumoniae* and zymosan (Zymo), which induces LAP (52), colocalized with both membrane (NOX2; $gp91^{phox}$) and cytosolic ($p40^{phox}$) components of the NADPH oxidase (Fig. 2 *A* and *B*) and that infection with *S. pneumoniae* triggered a significant increase in ROS (Fig. 2*C*). Pretreatment

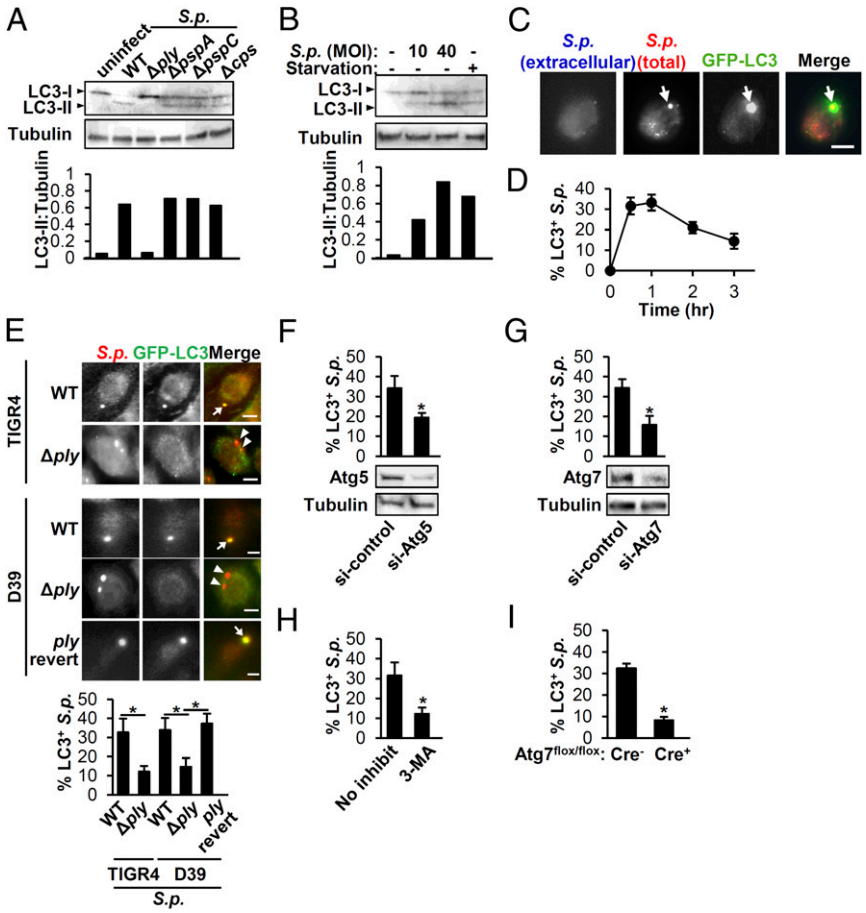

Fig. 1. *S.p.* triggers PLY-dependent LC3 conjugation and colocalization with internalized bacteria. (*A*) BMDMs treated with BafA1 were infected with indicated strains of *S.p.* for 1.5 h. Cell lysates were immunoblotted to detect LC3 or as a loading control tubulin. Densitometric quantification of LC3-II was normalized to tubulin. Data shown are representative of three experiments. (*B*) RAW264.7 macrophages treated with BafA1 were untreated, starved, or infected with *S.p.* at the designated MOI, as indicated, for 1.5 h. Cell lysates were immunoblotted to detect LC3 or tubulin. Densitometric quantification of LC3-II was normalized to tubulin. Data shown are representative of three experiments (*C* and *D*). (*C*) RAW264.7 macrophages stably expressing GFP-LC3 were infected with *S.p.* At 1 h postinfection, cells were stained to identify extracellular and total bacteria as described in *Methods*. Arrow: intracellular *S.p.* colocalized with LC3. (Scale bar, 5 μm.) Shown are representative of three experiments. (*D*) The percentage of intracellular *S.p.* that colocalized with LC3 was quantified at the indicated time points postinfection. Shown are the mean ± SEM of three independent experiments. (*E*) RAW264.7 macrophages stably expressing GFP-LC3 were infected with WT, pneumolysin-deficient (Δ*ply*) or a revertant with restored *ply* ("*ply* revert") *S.p.* strains for 1 h. Arrows: intracellular *S.p.* colocalized with LC3; arrowheads: intracellular *S.p.* not colocalized with LC3. (Scale bar, 5 μm.) Shown are representative of three experiments. The percentages of LC3$^+$ *S.p.* was quantified. Shown are the mean ± SEM of three independent experiments. *$P < 0.05$ by two-way ANOVA followed by the Bonferroni test. (*F* and *G*) RAW264.7 macrophages stably expressing GFP-LC3 were transfected with siRNA for the control, *Atg5* (*F*), or *Atg7* (*G*) for 48 h. Cell lysates were immunoblotted to detect Atg5, Atg7, or tubulin, with image representative of three independent experiments. Cells were infected with *S.p.* for 1 h, and the percentages of LC3$^+$ *S.p.* were quantified. Shown are the mean ± SEM of three independent experiments. * indicates $P < 0.05$ by Student's *t* test. (*H*) RAW264.7 macrophages stably expressing GFP-LC3 were untreated or pretreated with 3-MA for 0.5 h and then infected with *S.p.* for 1 h. The percentages of LC3$^+$ *S.p.* were quantified. Shown are the mean ± SEM of three independent experiments. * indicates $P < 0.05$ by Student's *t* test. (*I*) BMDMs isolated from *Atg7*-knockout (KO) (*Atg7*$^{flox/flox}$-LysM-Cre$^+$) or control (*Atg7*$^{flox/flox}$-LysM-Cre$^-$) mice were transfected with GFP-LC3 and then were infected with *S.p.* for 1 h. The percentage of LC3$^+$ *S.p.* was quantified. Data show mean ± SEM from one representative experiment from, at least, two independent experiments. *, $P <$ 0.05 by the Mann–Whitney *U* test. n.s., not significant; *S.p.*, *Streptococcus pneumoniae*.

of RAW264.7 cells with the NADPH oxidase inhibitor diphenyleneiodonium (DPI) significantly reduced LC3 recruitment to both Zymo and *S. pneumoniae* (Fig. 2*D*). Although PLY was required for the conversion of LC3-I to LC3-II (Fig. 1*A*) and for colocalization of LC3 with internalized *S. pneumoniae*, PLY is not required for ROS production (53). Here, we confirmed this result (*SI Appendix*, Fig. S2*A*) and further showed that PLY was also not required for bacterial colocalization with NOX2 (gp91^{phox}; *SI Appendix*, Fig. S2*B*), suggesting that *S. pneumoniae* may also trigger ROS production by mechanisms not related to phagosomal damage.

Next, we characterized the roles of several proteins that are differentially required for canonical autophagy and LAP for their involvement in LC3 recruitment to intracellular *S. pneumoniae* in BMDMs and RAW264.7 macrophages. First, in contrast to LAP, canonical autophagy requires inactivation of the mTOR pathway and results in dephosphorylation of the mTOR substrate p70S6K (54). Indeed, p70S6K was dephosphorylated in BMDMs treated with Rapa, a known inducer of canonical autophagy but not with exposure to Zymo or *S. pneumoniae* (Fig. 3*A*). In RAW264.7 cells, silencing of *Ulk1*, *FIP200*, and *Atg14*, all of which are required for canonical autophagy but not LAP, eliminated Rapa-induced autophagic responses as predicted (*SI Appendix*, Fig. S3 *A* and *B*) but did not affect LC3 colocalization with *S. pneumoniae* (Fig. 3 *B–D* and *SI Appendix*, Fig. S3 *C–E*). In contrast, silencing *Rubicon*, which is specifically required for LAP (52, 55, 56), did not impact Rapa-induced autophagy (*SI Appendix*, Fig. S3 *A* and *B*) but inhibited LC3 colocalization to *S.*

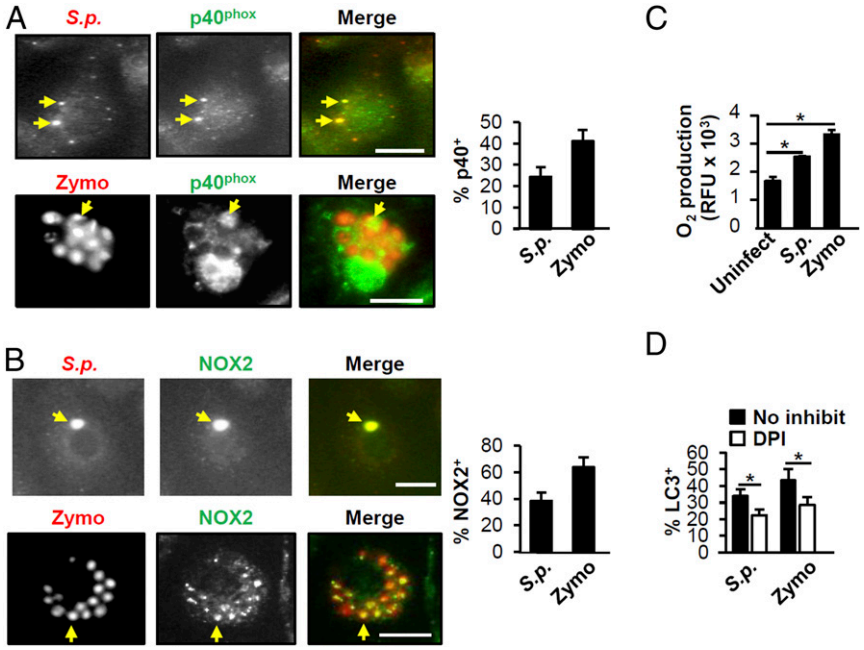

Fig. 2. *S.p.* triggers an increase in ROS production upon BMDM infection. (*A* and *B*) BMDMs were incubated with *S.p.* or Zymo for 1 h and subjected to immunofluorescence microscopy. Arrows indicate *S.p.* or Zymo colocalized with p40^{phox} (*A*) or NOX2 (gp91^{phox}) (*B*). (Scale bar, 5 μm.) The percentage of *S.p.* or Zymo that colocalized with p40^{phox} (*A*) or NOX2 (gp91^{phox}) (*B*) was quantified. Shown are the mean ± SEM from one representative experiment from, at least, two independent experiments. (*C*) BMDMs were treated with *S.p.* or 10-μg/mL Zymo for 1.5 h. The cells were stained with CellROX reagent. Fluorescense was read on a microplate reader. Shown are the mean ± SEM from one of three independent experiments. *$P < 0.05$ (Student's *t* test). (*D*) RAW264.7 macrophages stably expressing GFP-LC3 pretreated with or without 10-mM DPI were treated with *S.p.* or Zymo for 1 h. The percentage of LC3$^+$ *S.p.* or Zymo was quantified. Shown are the mean ± SEM of three independent experiments. *$P < 0.05$ by Student's *t* test. *S.p.*, *Streptococcus pneumoniae*.

pneumoniae (Fig. 3*B* and *SI Appendix*, Fig. S3*C*). Similarly, KO genes uniquely required for LAP, such as *Rubicon* and *Nox2* (54) significantly reduced LC3 recruitment to *S. pneumoniae*, whereas KO of *Atg14*, a gene essential for canonical autophagy only (54), did not (Fig. 3 *E* and *F* and *SI Appendix*, Fig. S3 *F* and *G*).

Lastly, in canonical autophagy, the cargo becomes entrapped inside double-membrane structures termed autophagosomes, whereas in LAP, the target is engulfed into single-membraned phagosomes (41). We assessed vesicle membrane structure by transmission electron microscopy. Whereas vesicles in Rapa-treated BMDMs exhibited double membranes, only single-membrane structures, indicative of LAP phagosomes, were found to contain Zymo and *S. pneumoniae* in BMDMs treated with the respective stimuli (Fig. 3*G* and *SI Appendix*, Table S1). Together, these results suggest that *S. pneumoniae* triggers LAP, not canonical autophagy, in BMDMs.

LAP Promotes Clearance of *S. pneumoniae*. LAP can result in delivery of microbes to lysosomes for subsequent degradation (38). We found that most LC3-positive *S. pneumoniae* vesicles also colocalized with lysosome-associated membrane protein 2 (LAMP-2) in BMDMs (Fig. 4*A*), indicating that this process often resulted in delivery of the bacteria to late endosomes or lysosomes. To determine whether LAP was important for killing internalized *S. pneumoniae* in BMDMs, we assessed *S. pneumoniae* survival in BMDMs and found that *S. pneumoniae* was killed in a time-dependent manner (Fig. 4*B*). To determine whether this killing was mediated by LAP, we evaluated *S. pneumoniae* killing in BMDMs lacking *Atg14*, *Atg7*, *Rubicon*, or *Nox2*. BMDMs lacking *Atg14*, which is required specifically for canonical autophagy, cleared *S. pneumoniae* as effectively as WT BMDMs (Fig. 4*C*). In contrast, those lacking *Atg7*, *Rubicon*, or *Nox2* were defective in *S. pneumoniae* clearance (Fig. 4 *D* and *E*). ROS have antibacterial effects against *S. pneumoniae* independent of LAP (42, 57). However, we did not observe additional killing defects in in *Nox2*$^{-/-}$ BMDMs compared to LAP defective *Rubicon*$^{-/-}$ BMDMs (Fig. 4*E*). Although *Rubicon*$^{-/-}$ BMDMs are somewhat diminished in ROS production upon challenge with Zymo due to the role of Rubicon in stabilizing NOX2 NADPH oxidase (52), these results suggest that the primary mechanism of *S. pneumoniae* killing in BMDMs depends on ROS-mediated LAP rather than the direct bacteriocidal activity of ROS.

***S. pneumoniae*-Triggered LAP Is Impaired in Aged BMDMs.** Autophagic activities tend to decline with age (58). As the elderly population is especially susceptible for *S. pneumoniae* infection, we set out to examine whether BMDMs from young and aged mice differ in *S. pneumoniae*-triggered LAP. We transfected BMDMs isolated from young (2-mo old) and aged (20- to 22-mo old) with GFP-LC3 and confirmed that young and aged BMDMs displayed no difference in transfection efficiency or posttransfection cell viability (*SI Appendix*, Fig. S4). In addition, although *S. pneumoniae* has been reported to induce cytotoxicity in BMDMs upon extended (4-h) infection by an MOI of 100 (59), we confirmed no LDH release by young or aged BMDMs upon pneumococcal infection at an MOI of 50 for 80 min. Upon *S. pneumoniae* infection of GFP-LC3-expressing cells, colocalization was significantly higher in young BMDMs than aged BMDMs throughout the 3-h time course (Fig. 5 *A* and *B*). Immunoblotting for LC3 revealed a twofold increase in LC3-II conversion in *S. pneumoniae*-infected young BMDMs compared to uninfected control as early as 1.5-h postinfection, whereas infected aged BMDMs responded with no significant increase in LC3-II even after 3 h of infection (Fig. 5*C*). That both LC3 conversion and recruitment are significantly lower in aged BMDMs suggests that LAP is more efficiently triggered by *S. pneumoniae* infection in young BMDMs compared to aged BMDMs. This relative defect in *S. pneumoniae*-triggered LAP was

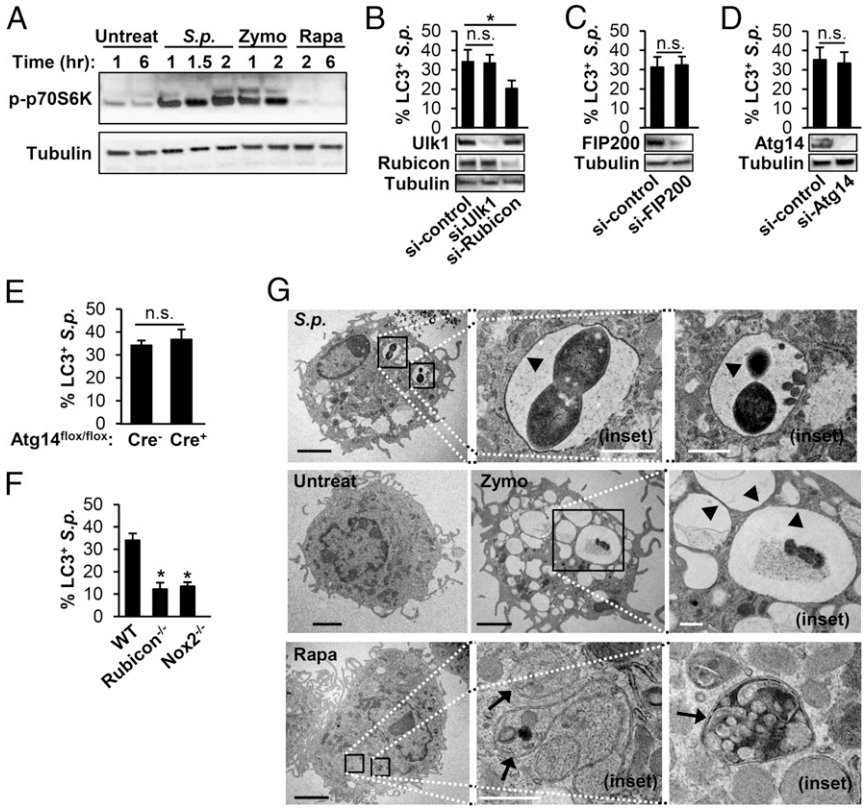

Fig. 3. *S.p.* triggers LAP and not canonical autophagy in primary murine BMDMs. (*A*) BMDMs from WT mice were untreated, infected with *S.p.*, or treated with 10-μg/mL Zymo or 200-nM Rapa for the indicated periods. Cell lysates were immunoblotted to detect p-p70S6K and tubulin. Data are representative of three independent experiments. (*B–D*) RAW264.7 macrophages stably expressing GFP-LC3 were transfected with control siRNA, *Ulk1* siRNA, or *Rubicon* siRNA (*B*); control siRNA or *FIP200* siRNA (*C*); control siRNA or *Atg14* siRNA (*D*) for 48 h. These cells were treated with *S.p*. Cell lysates were immunoblotted to detect Ulk1, Rubicon, FIP200, Atg14, or tubulin. The percentage of $LC3^+$ *S.p.* was quantified. *$P < 0.05$, one-way ANOVA with Dunnett's test. (*E* and *F*) BMDMs isolated from *Atg14*-KO ($Atg14^{flox/flox}$-LysM-Cre^+) or control ($Atg14^{flox/flox}$-LysM-Cre^-) mice (*E*); WT, $Rubicon^{-/-}$, and $Nox2^{-/-}$ (*F*) were transfected with GFP-LC3 and then were infected with *S.p.* for 1 h. The percentage of $LC3^+$ *S.p.* was quantified. Data shown mean ± SEM from one representative experiment from, at least, two independent experiments. *, $P < 0.05$ by the Mann–Whitney *U* test. n.s.. (*G*) BMDMs were untreated or infected with *S.p.* for 40 min or treated with 10-μg/mL Zymo for 40 min or 200-nM Rapa for 6 h and subjected to transmission electron microscopy. Images are representative of three experiments. Arrowheads indicate single membrane; arrows indicate double membrane. The magnified insets represents the area indicated by the squares. (Black scale bar: 2 μm; white scale bar: 500 nm.) n.s., not significant; *S.p.*, *Streptococcus pneumoniae*.

not due to a defect in ROS production because young and aged BMDMs produced equivalent amounts (*SI Appendix*, Fig. S5).

To determine if the decline in LAP in aged BMDMs compromised the ability of aged BMDMs to kill internalized *S. pneumoniae*, we measured killing of *S. pneumoniae* by BMDMs from young or aged mice over time. Compared to young BMDMs, aged BMDMs were consistently less efficient at clearing *S. pneumoniae* over the 120-min period examined (Fig. 6*A*). We found that silencing of *Rubicon* in young BMDMs resulted in a twofold increase in the survival of *S. pneumoniae*, but had no effect on the ability of aged BMDMs to kill the bacterium (Fig. 6*B*), suggesting that LAP contributes to pneumococcal killing by young BMDM and that the relative defect of *S. pneumoniae*-induced LAP in aged BMDM is associated with a relative defect in bacterial killing.

LAP is immunomodulatory (39) and aging is associated with higher basal and induced levels of proinflammatory cytokines (28). In addition, in response to 24 h of infection by *S. pneumoniae*, aged mice produce higher levels of *Il6*, *Tnf*, and *Il1b* messenger RNA (mRNA) (35). We utilized qRT-PCR to quantitate the level of induction of these cytokine mRNAs upon a 90-min infection by *S. pneumoniae* in young or aged BMDMs that had been subjected to control small interfering RNA (siRNA) or *Rubicon* siRNA to diminish LAP. After infection, control siRNA-treated aged BMDMs produced higher levels of *Il6*, *Tnf*, and *Il1b* compared to control siRNA-treated young BMDMs, consistent with inflammaging. In young BMDMs infected with *S. pneumoniae*, inhibition of LAP by silencing of *Rubicon* increased cytokine production to levels indistinguishable from those of the aged BMDMs, indicating that LAP as predicted functions to diminish inflammatory cytokine gene expression. In contrast, LAP inhibition in aged BMDMs had no effect on the production of *Il6*, *Tnf*, or *Il1b*, consistent with our previous finding that BMDMs LAP is significantly diminished by aging (Fig. 7). PLY-deficient *S. pneumoniae* were found to induce levels of *Il6*, *Tnf*, and *Il1b* statistically indistinguishable from those induced by WT bacteria (53), a result we confirmed here (*SI Appendix*, Fig. S6), indicating that PLY deficiency may trigger alternate pathways of cytokine production that are not influenced by autophagic processes. Nevertheless, our findings with *Rubicon* siRNA indicate that the decline in a LAP response triggered by infection of aged BMDMs with WT *S. pneumoniae* not only reduced killing of *S. pneumoniae*, but also increased expression of genes encoding proinflammatory cytokines.

Discussion

In this study, we investigated the interaction of pneumococcus with BMDMs, which play a critical role in host defense against *S. pneumoniae* disease. We found that, upon infection of either murine BMDMs or a macrophage line, *S. pneumoniae* triggered LC3 recruitment in a manner dependent upon the pore-forming toxin PLY. In cultured epithelial cells and fibroblasts, *S. pneumoniae* has

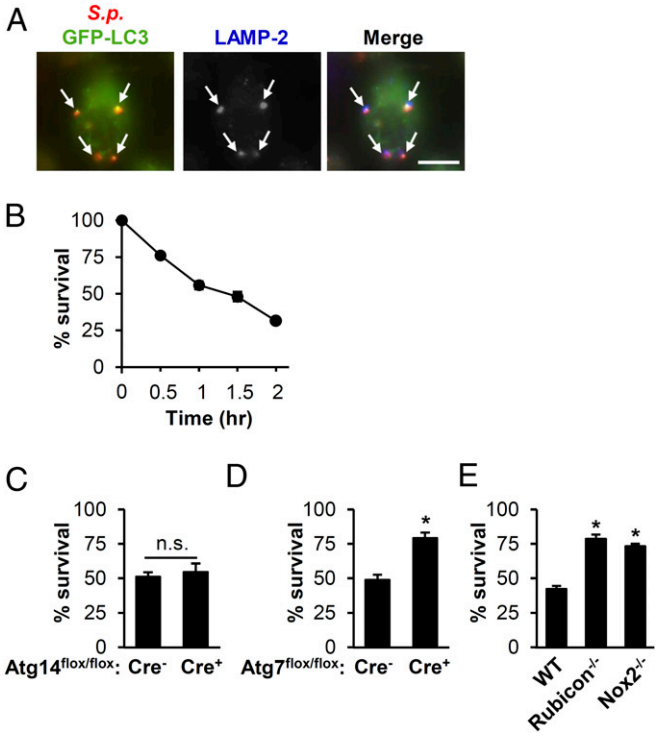

Fig. 4. LAP contributes to clearance of *S.p.* by BMDMs. (*A*) BMDMs transfected with GFP-LC3 were infected with *S.p.* At 1-h postinfection, cells were stained for *S.p.*, LC3, and LAMP-2. Shown are images representative of three independent experiments. Arrows: *S.p.* colocalized with LC3 and LAMP-2. (Scale bar, 5 μm.) (*B*) Survival of *S.p.* in BMDMs from young WT mice. Data show the mean ± SEM of a representative experiment from, at least, three independent experiments. (*C*–*E*) The percent *S.p.* survival was determined after 1.5-h infection of BMDMs from *Atg14*-KO (*Atg14*$^{flox/flox}$-LysM-Cre^{+}) or control (*Atg14*$^{flox/flox}$-LysM-Cre^{-}) mice (*C*); *Atg7*-KO (*Atg7*$^{flox/flox}$-LysM-Cre^{+}) or control (*Atg7*$^{lox/flox}$-LysM-Cre^{-}) (*D*); WT, *Rubicon*$^{-/-}$, or *Nox2*$^{-/-}$ (*E*). Data show mean ± SEM from a representative experiment from, at least, two independent experiments. *, $P < 0.05$ by the Mann–Whitney *U* test. n.s., not significant; *S.p.*, *Streptococcus pneumoniae*.

been shown to elicit autophagy in a PLY-dependent manner (44–46). Endosomal membrane disruption is one trigger for autophagy activation (60), and several other bacteria that produce membrane-damaging toxins, including *Shigella flexneri*, *Salmonella enterica*, *Vibrio cholerae*, *Listeria monocytogenes*, and *Staphylococcus aureus*, induce autophagy (45, 61–64). Group A *Streptococcus* encodes streptolysin O (SLO), a cholesterol-dependent cytolysin highly related to PLY, that similarly triggers an autophagic process (65). Although PLY, unlike SLO (66), lacks a canonical secretion signal, it is localized to the bacterial surface and can also be released upon bacterial lysis (67–70). In BMDMs, we also found a role for PLY, but in this case, *S. pneumoniae* activated LAP. In addition, autophagy and autophagy-related processes can be activated by cell surface and endosomal pattern recognition receptors, such as Toll-like receptors (TLRs) (41, 71), and PLY (72) as well as other pneumococcal factors (6) have been reported to interact with TLR2 and TLR4. PLY binds to macrophages and dendritic cell mannose receptor C type I (73), a phagocytic receptor that is implicated in enhancing a number of macrophage antimicrobial functions, including autophagy (74). Whether PLY engagement of pattern recognition receptors contributes to LC3 trafficking pathways will require further investigation.

Several studies have indicated that in fibroblasts or epithelial cells, *S. pneumoniae* triggers a canonical autophagic process that requires factors, such as *FIP200* and *Ulk1*, that are dispensable for LAP, and results in the engulfment of the bacterium in double-membrane autophagosomes (46, 51). Treatment of mice with Rapa to induce canonical autophagy results in modest protection from *S. pneumoniae* lung challenge but is not associated with reduced lung burden (75). We found that *S. pneumoniae* internalized into BMDMs colocalize with LC3 in a fashion requiring *Atg5* and *Atg7*, two components of the autophagic machinery (48) that are required for both canonical autophagy and LAP. We developed evidence that in BMDMs, the pathogen triggers LAP rather than canonical autophagy. p70S6K, a substrate of mammalian target of Rapa (mTOR) and, hence, a protein that is dephosphorylated during metabolically regulated canonical autophagy, remained phosphorylated in *S. pneumoniae*-infected BMDMs. Although LC3 recruitment during LAP is reliant on several autophagy proteins, such as *Atg5* and *Atg7*, it is characterized by its independence from components of the autophagy preinitiation complex, such as *Ulk1*, *Atg13*, and *FIP200* (52), or components of the initiation complex for canonical autophagy, such as *Atg14*. We found that depletion of *Ulk1* or *FIP200*, or depletion or genetic ablation of *Atg14*, had no effect on LC3 recruitment to *S. pneumoniae*, whereas depletion and/or ablation of autophagic components specific to LAP, such as *Rubicon* or *Nox2*, diminished LC3 recruitment more than twofold. Reflecting a functional role of the NADPH oxidase, *S. pneumoniae*-infected BMDMs generated ROS, a necessary step for LAP but not canonical autophagy, and chemical inhibition of ROS production blocked recruitment of LC3 to pneumococcus-containing phagosomes. Finally, internalized *S. pneumoniae* were sequestered within single- rather than double-membrane structures, consistent with LAP. Thus, pharmacological inhibition, genetic silencing and ablation, and morphological analyses indicate that *S. pneumoniae* trigger LAP in BMDMs.

A common method of assessing autophagy, particularly, before the widespread recognition of LAP as an important means of antimicrobial defense, has been the detection of pathogen-associated LC3 puncta (36). LC3 localization is associated with both LAP and

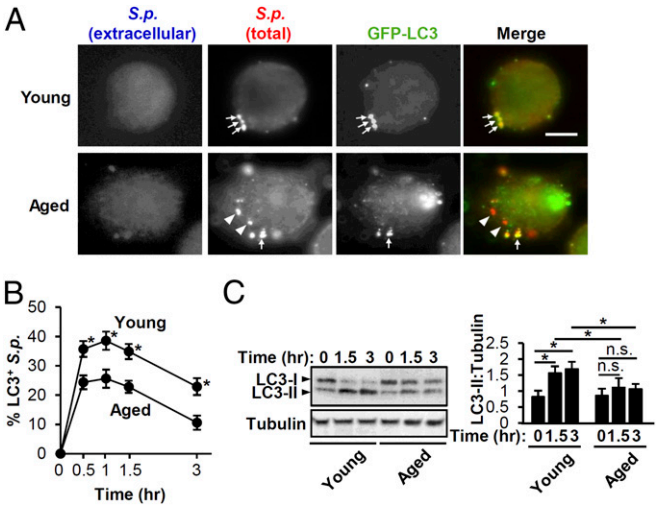

Fig. 5. LC3 conjugation and localization to *S.p.* is impaired in aged BMDMs. (*A*) Immunofluorescent (IF) images of LC3 and *S.p.* at 1-h postinfection in BMDMs from young and aged mice otransfected with GFP-LC3. Shown are representative of three experiments. Arrows: intracellular *S.p.* colocalized with LC3; arrowheads: intracellular *S.p.* not colocalized with LC3. (Scale bar, 5 μm.) (*B*) The percentage of LC3^{+} *S.p.* was quantified. Shown are the mean ± SEM of three independent experiments. *, $P < 0.05$ by the Mann–Whitney *U* test. (*C*) BMDMs from young and aged mice were uninfected or infected with *S.p.* for the indicated periods. Cell lysates were immunoblotted to detect LC3 or tubulin with image representative of three experiments. Densitometric quantification of LC3-II was normalized to tubulin. Shown are the mean ± SEM of three independent experiments. *, $P < 0.05$; n.s. by two-way ANOVA followed by the Bonferroni test. n.s., not significant; *S.p.*, *Streptococcus pneumoniae*.

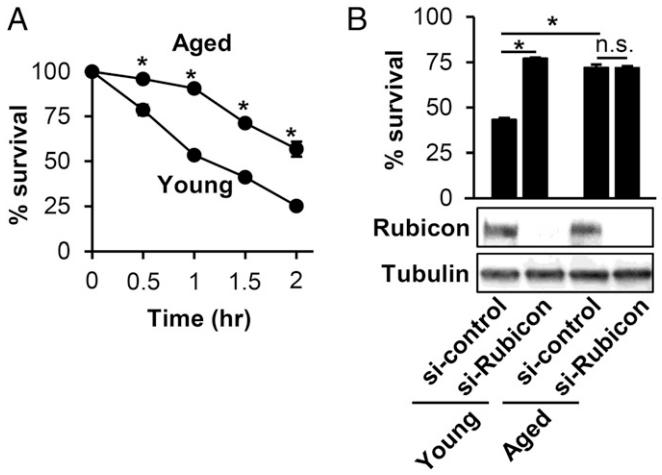

Fig. 6. *S.p.* survival is enhanced by inhibition of LAP in young but not aged BMDMs. (*A*) Survival of *S.p.* in young and aged BMDMs. Data show the mean ± SEM of one representative experiment from, at least, three independent experiments. $*P < 0.05$ by the Mann–Whitney *U* test. (*B*) BMDMs from young and aged mice were transfected with control siRNA or *Rubicon* siRNA for 48 h. Cell lysates were immunoblotted to detect Rubicon or tubulin with image representative of three experiments. These cells were infected with *S.p.* for 1.5 h. The percent survival after 1.5-h infection compared to 0 min was calculated. Data show the mean ± SEM of one representative experiment from three independent experiments. $*P < 0.05$ by two-way ANOVA followed by the Bonferroni test. n.s., not significant; *S.p.*, *Streptococcus pneumoniae*.

canonical autophagy, and the emergence of facile methods to distinguish LAP from canonical autophagy only relatively recently raised the possibility that LAP occurs in cell types other than macrophages. For example, high levels of ROS are generated upon pneumococcal infection of A549 cells, and inhibition of ROS production decreases autophagy and enhances bacteria survival (51). In addition, in mouse embryo fibroblasts (MEFs), *S. pneumoniae* triggers canonical autophagy only after initially activating a process that resembles LAP in its independence of FIP200 and Ulk1 (47). However, this early LC3 trafficking in MEFs requires neither PI3 kinase activity nor ROS production, hallmarks of conventional LAP (48, 52). Furthermore, in contrast to the bacteriocidal process described here in BMDM (Fig. 4), MEF-mediated bacterial killing required further processing to autophagosomes by components of the canonical autophagic machinery, such as ATG14 (47). The relationship of the noncanonical autophagy pathway in MEFs to LAP in BMDMs described here and the mechanisms resulting in the disparate fates of internalized bacteria remain to be explored. The specialized phagocytic nature of macrophages, for example, in higher levels of NOX2 compared to fibroblasts (76), the degree of phagosomal acidification, or the production of serine proteases (77) or antimicrobial peptides (78) may result in their alternate autophagic responses and subsequent bacteriocidal efficacy (38).

Recruitment of inflammatory cells, including macrophages, to the lungs during *S. pneumoniae* infection is increased in aged compared to young mice (79) and is associated with greater bacterial burden, raising the possibility that aged macrophages may be compromised in both effector and immunomodulatory function. Autophagic capacity declines with age, contributing to many of the diseases associated with advanced age (58). A number of common age-related cellular senescence pathways, such as those that increase mitochondrial or endoplasmic reticulum stress, not only regulate autophagic processes by a myriad of mechanisms (80–82), but also have been shown to functionally impair macrophage responses to *S. pneumoniae* (35, 79, 83). Aging is associated with diminished expression of several autophagy proteins, including those, such as ATG5 and ATG7, that function in both canonical autophagy and LAP (54). We observed no striking difference in the level of Rubicon produced by young or aged BMDM (Fig. 6*B*); previous studies suggest that age-related differences in Rubicon expression may differ depending upon tissue type (84, 85). Regardless, in our functional studies, we found that *S. pneumoniae*-induced LAP, reflected in the conjugation of LC3 and its colocalization with ingested bacteria, diminished with age. Bacteriocidal activity was correspondingly compromised in aged BMDMs, and in contrast to young BMDMs, unaffected by LAP inhibition. Similarly, aged BMDMs were more highly inflammatory than young BMDMs, reflected in higher levels of proinflammatory cytokine expression after *S. pneumoniae* infection. The relatively muted inflammatory response of young compared to aged BMDMs was due to LAP because LAP inhibition enhanced their response. In contrast, the expression of inflammatory cytokines after infection of aged (and relatively LAP-deficient) BMDMs was unaffected by LAP inhibition.

Human monocyte-derived macrophages from frail elderly individuals exhibit a significant defect in controlling *S. pneumoniae* (86). The precise nature of this defect remains unclear, but LAP-mediated defense has been demonstrated to be critical to host defense against a variety of infectious agents, several of which cause more serious infection in aged individuals. For example, adults older than 65 y are at increased risk of serious food-borne illness caused by *L. monocytogenes* or *S. enterica* (87), two pathogens for which LAP functions to mitigate systemic infection (88–90). Moreover, the regulatory effect of LAP on production of proinflammatory cytokines would be predicted to modulate intestinal proliferation of *S. enterica* for which growth is metabolically promoted by a robust inflammatory response (91). Among other lung pathogens, *Legionella pnemophila* and *Mycobacterium tuberculosis* cause more severe illness in the aged (92, 93) and are capable of triggering LAP (94). Several of the above pathogens are capable of manipulating LAP or LAP-like pathways (61, 62, 95–97), a property that may render elderly individuals, who may have a preexisting partial defect in LAP, particularly, susceptible to these infections. Thus, our finding that LAP is an important innate immune defense employed by BMDMs to control both *S. pneumoniae* infection and concomitant inflammation, one that diminishes with age, may provide insight into to the age-related susceptibility to diverse microbial pathogens.

Materials and Methods

Reagents. Rapa, 3-MA, DPI, and digitonin were obtained from Millipore Sigma.

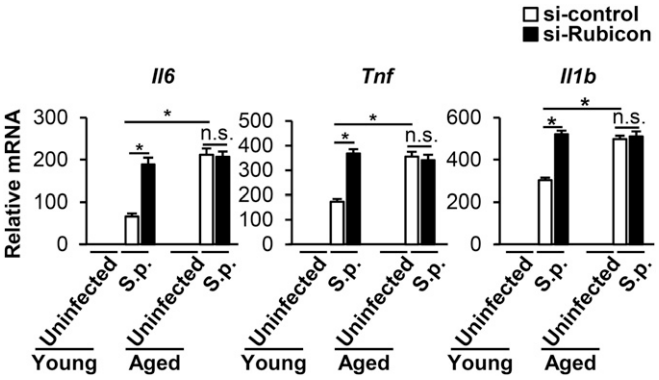

Fig. 7. *S.p.* cytokine responses are enhanced by inhibition of LAP in young but not aged BMDMs. siRNA-transfected BMDMs were infected with *S.p.* for 1.5 h. RNA was extracted and the levels of cytokines relative to young uninfected BMDM transfected with control siRNA were determined by qRT-PCR. Shown are the mean ± SEM of one of three independent experiments. $*P < 0.05$ by two-way ANOVA followed by the Bonferroni test. *S.p.*, *Streptococcus pneumoniae*.

Bacterial Strains and Mutants. *S. pneumoniae* TIGR4 (serotype 4) was used as a WT strain in this study. The TIGR4 mutant strains, including Δ*cps*, Δ*ply*, Δ*pspA*, and Δ*pspC* were provided by Professor A. Camilli (Tufts University, Boston, MA). The *S. pneumoniae* D39 (serotype 2), D39 mutant strain that lacks PLY (D39Δ*ply*), and D39Δ*ply* complemented with PLY (D39Δ*ply ply* comp) were described previously (24). These *S. pneumoniae* strains were grown as described in the *SI Appendix*, SI Materials and Methods.

Mice. Young (2-mo) and aged (22–26-mo) male C57BL/6 mice were purchased from Charles River Laboratories and the National Institute on Aging rodent facility. *Atg7*$^{flox/flox}$*-LysM-Cre* and *Atg14*$^{flox/flox}$*-LysM-Cre* were generously provided by H. W. Virgin (Washington University School of Medicine [WUSM]). *Rubicon*$^{-/-}$ mice were provided by D. Young (St. Jude Children's Research Hospital, Memphis, TN). *Nox2*-KO mice were provided by M. Dinauer (WUSM). All mice were maintained in a specific-pathogen free facility at Tufts University, Gifu University, and Washington University, and all procedures were performed in accordance with Institutional Animal Care and Use Committee guidelines. No animals were used in the study if they had evidence of visible skin lesions, weight loss, or lymphadenopathy.

BMDMs and Mouse RAW264.7 Cells. The phenotype of BMDM induced to differentiate with granulocyte-macrophage colony-stimulating factor (GM-CSF) resembles that of macrophages recruited to lungs (98), and we harvested bone-marrow cells from the femurs and tibiae of male C57BL/6 mice, followed by incubation in differentiation medium, i.e., basal medium with GM-CSF. BMDMs and RAW264.7 cells (American Type Culture Collection) were grown as described in the *SI Appendix*, SI Materials and Methods.

Plasmids, siRNA, and Transfection. pGFP-LC3 was a gift from T. Yoshimori (Addgene plasmid no. 21073) (99). Stealth predesigned siRNAs and the control nontargeting siRNA (negative control med GC) were acquired from Thermo Fisher Scientific. Transfection was performed as described in the *SI Appendix, SI Materials and Methods*.

Western Blotting. Western blotting was performed as described in the *SI Appendix, SI Materials and Methods*.

Electron Microscopy. Electron microscopy was performed as described in the *SI Appendix, SI Materials and Methods*.

Bacterial Killing Assay. To measure BMDM killing of *S. pneumoniae*, 5×10^5 BMDMs were preincubated with an MOI of 10 bacteria per BMDM for 1 h at 37 °C with gentle inversion as outlined above to allow for internalization of bacteria (34). Viable colony-forming units were determined by culturing of supernatants on TS agar plates.

Immunofluorescence. Cells (2×10^5 cells/well) were seeded on 4- or 8-well Permanox slides (Nunc Lab-Tek Chamber Slide System; Thermo Fisher Scientific). The following day, they were infected with *S. pneumoniae* at an MOI of 20 for 1 h, washed with phosphate-buffered saline (PBS) three times, and fixed with 4% paraformaldehyde in PBS for 10 min at 37 °C. To distinguish between intracellular and extracellular *S. pneumoniae*, extracellular and total bacteria were differentially stained as described previously (100). Immunostaining and image acquisition were performed as described in the *SI Appendix, SI Materials and Methods*.

Detection of ROS. CellROX reagents for oxidative stress detection (C10448; Thermo Fisher Scientific) was performed according to the protocol.

RNA Isolation and qRT-PCR. RNA isolation and qRT-PCR were performed as described in the *SI Appendix, SI Materials and Methods*.

Statistics. Data are shown as the mean ± SEM. For single comparisons, P values were calculated using the Mann–Whitney U test or Student's t test. For multiple comparisons, two-way ANOVA followed by a Bonferroni test or one-way ANOVA with Dunnett's test were used. Differences with $P < 0.05$ were considered significant.

Data Availability. All study data are included in the article and supporting information.

ACKNOWLEDGMENTS. We thank Elsa Bou Ghanem, Sara Roggensack, Marcia Osburne, Nalat Siwapornchai, and Dawn Bowdish for helpful experimental advice and/or invaluable discussion in the preparation of the paper; H. W. Virgin (WUSM), M. Dinauer (WUSM), and D. Young (St. Jude Children's Research Hospital, Memphis, TN) for their generosity in providing mice; Hitoshi Iwahashi (Gifu University) for mouse experiment cooperation; and Greg Hendricks and Lara Strittmatter at the UMass Medical School Electron Microscopy Core for technical advice. This work was supported by a Grant-in-Aid for Scientific Research (KAKENHI) from the Japan Society for the Promotion of Science to M.I. (18K09544), the Pott's Memorial Foundation to P.C., and NIH/National Institute of Allergy and Infectious Diseases R01s (Grant AI087682, Grant AI130454) to J.A.P.

1. D. Bogaert, R. De Groot, P. W. Hermans, *Streptococcus pneumoniae* colonisation: The key to pneumococcal disease. *Lancet Infect. Dis.* **4**, 144–154 (2004).
2. T. van der Poll, S. M. Opal, Pathogenesis, treatment, and prevention of pneumococcal pneumonia. *Lancet* **374**, 1543–1556 (2009).
3. N. Miyashita, Y. Yamauchi, Bacterial pneumonia in elderly Japanese populations. *Jpn. Clin. Med.* **9**, 1179670717751433 (2018).
4. J. Xu, S. L. Murphy, K. D. Kochanek, B. Bastian, E. Arias, Deaths: Final data for 2016. *Natl. Vital Stat. Rep.* **67**, 1–76 (2018).
5. J. Cole, J. Aberdein, J. Jubrail, D. H. Dockrell, The role of macrophages in the innate immune response to *Streptococcus pneumoniae* and Staphylococcus aureus: Mechanisms and contrasts. *Adv. Microb. Physiol.* **65**, 125–202 (2014).
6. U. Koppe, N. Suttorp, B. Opitz, Recognition of *Streptococcus pneumoniae* by the innate immune system. *Cell. Microbiol.* **14**, 460–466 (2012).
7. C. L. Krone, K. Trzciński, T. Zborowski, E. A. Sanders, D. Bogaert, Impaired innate mucosal immunity in aged mice permits prolonged *Streptococcus pneumoniae* colonization. *Infect. Immun.* **81**, 4615–4625 (2013).
8. S. E. Evans, D. E. Ost, Pneumonia in the neutropenic cancer patient. *Curr. Opin. Pulm. Med.* **21**, 260–271 (2015).
9. M. Arredouani *et al.*, The scavenger receptor MARCO is required for lung defense against pneumococcal pneumonia and inhaled particles. *J. Exp. Med.* **200**, 267–272 (2004).
10. M. S. Arredouani *et al.*, The macrophage scavenger receptor SR-AI/II and lung defense against pneumococci and particles. *Am. J. Respir. Cell Mol. Biol.* **35**, 474–478 (2006).
11. L. A. Sanders *et al.*, Fc gamma receptor IIa (CD32) heterogeneity in patients with recurrent bacterial respiratory tract infections. *J. Infect. Dis.* **170**, 854–861 (1994).
12. S. Weber, H. Tian, N. van Rooijen, L. A. Pirofski, A serotype 3 pneumococcal capsular polysaccharide-specific monoclonal antibody requires Fcγ receptor III and macrophages to mediate protection against pneumococcal pneumonia in mice. *Infect. Immun.* **80**, 1314–1322 (2012).
13. J. A. Preston *et al.*, Alveolar macrophage apoptosis-associated bacterial killing helps prevent murine pneumonia. *Am. J. Respir. Crit. Care Med.* **200**, 84–97 (2019).
14. D. H. Dockrell *et al.*, Alveolar macrophage apoptosis contributes to pneumococcal clearance in a resolving model of pulmonary infection. *J. Immunol.* **171**, 5380–5388 (2003).
15. D. H. Dockrell, M. K. B. Whyte, T. J. Mitchell, Pneumococcal pneumonia: Mechanisms of infection and resolution. *Chest* **142**, 482–491 (2012).
16. K. Taut *et al.*, Macrophage turnover kinetics in the lungs of mice infected with *Streptococcus pneumoniae*. *Am. J. Respir. Cell Mol. Biol.* **38**, 105–113 (2008).
17. D. Kafka *et al.*, Contribution of IL-1 to resistance to *Streptococcus pneumoniae* infection. *Int. Immunol.* **20**, 1139–1146 (2008).
18. K. Takashima *et al.*, Role of tumor necrosis factor alpha in pathogenesis of pneumococcal pneumonia in mice. *Infect. Immun.* **65**, 257–260 (1997).
19. F. Xu *et al.*, Modulation of the inflammatory response to *Streptococcus pneumoniae* in a model of acute lung tissue infection. *Am. J. Respir. Cell Mol. Biol.* **39**, 522–529 (2008).
20. E. Calbo, J. Garau, Of mice and men: Innate immunity in pneumococcal pneumonia. *Int. J. Antimicrob. Agents* **35**, 107–113 (2010).
21. I. Sohail, S. Ghosh, S. Mukundan, S. Zelewski, M. N. Khan, Role of inflammatory risk factors in the pathogenesis of *Streptococcus pneumoniae*. *Front. Immunol.* **9**, 2275 (2018).
22. R. J. José *et al.*, Regulation of neutrophilic inflammation by proteinase-activated receptor 1 during bacterial pulmonary infection. *J. Immunol.* **194**, 6024–6034 (2015).
23. R. Bhowmick, S. Clark, J. V. Bonventre, J. M. Leong, B. A. McCormick, Cytosolic phospholipase $A_2\alpha$ promotes pulmonary inflammation and systemic disease during Streptococcus pneumoniae infection. *Infect. Immun.* **85**, e00280-17 (2017).
24. R. Bhowmick *et al.*, Systemic disease during *Streptococcus pneumoniae* acute lung infection requires 12-lipoxygenase-dependent inflammation. *J. Immunol.* **191**, 5115–5123 (2013).
25. E. N. Bou Ghanem *et al.*, Extracellular adenosine protects against *Streptococcus pneumoniae* lung infection by regulating pulmonary neutrophil recruitment. *PLoS Pathog.* **11**, e1005126 (2015).
26. M. Daigneault *et al.*, Monocytes regulate the mechanism of T-cell death by inducing Fas-mediated apoptosis during bacterial infection. *PLoS Pathog.* **8**, e1002814 (2012).
27. S. Knapp *et al.*, Alveolar macrophages have a protective antiinflammatory role during murine pneumococcal pneumonia. *Am. J. Respir. Crit. Care Med.* **167**, 171–179 (2003).
28. C. Franceschi *et al.*, Inflamm-aging. An evolutionary perspective on immunosenescence. *Ann. N. Y. Acad. Sci.* **908**, 244–254 (2000).
29. A. R. Boyd, C. J. Orihuela, Dysregulated inflammation as a risk factor for pneumonia in the elderly. *Aging Dis.* **2**, 487–500 (2011).
30. I. M. Rea *et al.*, Age and age-related diseases: Role of inflammation triggers and cytokines. *Front. Immunol.* **9**, 586 (2018).
31. H. Bruunsgaard, P. Skinhøj, J. Qvist, B. K. Pedersen, Elderly humans show prolonged in vivo inflammatory activity during pneumococcal infections. *J. Infect. Dis.* **180**, 551–554 (1999).

32. E. N. Bou Ghanem *et al*., The alpha-tocopherol form of vitamin E boosts elastase activity of human PMNs and their ability to kill *Streptococcus pneumoniae*. *Front. Cell. Infect. Microbiol.* **7**, 161 (2017).
33. A. E. Williams, R. J. José, J. S. Brown, R. C. Chambers, Enhanced inflammation in aged mice following infection with *Streptococcus pneumoniae* is associated with decreased IL-10 and augmented chemokine production. *Am. J. Physiol. Lung Cell. Mol. Physiol.* **308**, L539–L549 (2015).
34. N. Thevaranjan *et al*., Age-associated microbial dysbiosis promotes intestinal permeability, systemic inflammation, and macrophage dysfunction. *Cell Host Microbe* **21**, 455–466.e4 (2017).
35. S. J. Cho, K. Rooney, A. M. K. Choi, H. W. Stout-Delgado, NLRP3 inflammasome activation in aged macrophages is diminished during *Streptococcus pneumoniae* infection. *Am. J. Physiol. Lung Cell. Mol. Physiol.* **314**, L372–L387 (2018).
36. M. D. Keller, V. J. Torres, K. Cadwell, Autophagy and microbial pathogenesis. *Cell Death Differ.* **27**, 872–886 (2020).
37. S. Upadhyay, J. A. Philips, LC3-associated phagocytosis: Host defense and microbial response. *Curr. Opin. Immunol.* **60**, 81–90 (2019).
38. M. Herb, A. Gluschko, M. Schramm, LC3-associated phagocytosis - the highway to hell for phagocytosed microbes. *Semin. Cell Dev. Biol.* **101**, 68–76 (2020).
39. B. L. Heckmann, E. Boada-Romero, L. D. Cunha, J. Magne, D. R. Green, LC3-Associated phagocytosis and inflammation. *J. Mol. Biol.* **429**, 3561–3576 (2017).
40. N. Mizushima, M. Komatsu, Autophagy: Renovation of cells and tissues. *Cell* **147**, 728–741 (2011).
41. M. A. Sanjuan *et al*., Toll-like receptor signalling in macrophages links the autophagy pathway to phagocytosis. *Nature* **450**, 1253–1257 (2007).
42. J. Huang *et al*., Activation of antibacterial autophagy by NADPH oxidases. *Proc. Natl. Acad. Sci. U.S.A.* **106**, 6226–6231 (2009).
43. J. Henault *et al*., Noncanonical autophagy is required for type I interferon secretion in response to DNA-immune complexes. *Immunity* **37**, 986–997 (2012).
44. P. Li *et al*., *Streptococcus pneumoniae* induces autophagy through the inhibition of the PI3K-I/Akt/mTOR pathway and ROS hypergeneration in A549 cells. *PLoS One* **10**, e0122753 (2015).
45. J. Mathieu, Interactions between autophagy and bacterial toxins: Targets for therapy? *Toxins* **7**, 2918–2958 (2015).
46. M. Ogawa *et al*., Molecular mechanisms of *Streptococcus pneumoniae*-targeted autophagy via pneumolysin, Golgi-resident Rab41, and Nedd4-1-mediated K63-linked ubiquitination. *Cell. Microbiol.* **20**, e12846 (2018).
47. M. Ogawa *et al*., *Streptococcus pneumoniae* triggers hierarchical autophagy through reprogramming of LAPosome-like vesicles via NDP52-delocalization. *Commun. Biol.* **3**, 25 (2020).
48. S. C. Lai, R. J. Devenish, LC3-Associated phagocytosis (LAP): Connections with host autophagy. *Cells* **1**, 396–408 (2012).
49. N. Mizushima, T. Yoshimori, How to interpret LC3 immunoblotting. *Autophagy* **3**, 542–545 (2007).
50. Z. Shu *et al*., *Streptococcus pneumoniae* PepO promotes host anti-infection defense via autophagy in a Toll-like receptor 2/4 dependent manner. *Virulence* **11**, 270–282 (2020).
51. A. Martner, C. Dahlgren, J. C. Paton, A. E. Wold, Pneumolysin released during *Streptococcus pneumoniae* autolysis is a potent activator of intracellular oxygen radical production in neutrophils. *Infect. Immun.* **76**, 4079–4087 (2008).
52. J. Martinez *et al*., Molecular characterization of LC3-associated phagocytosis reveals distinct roles for Rubicon, NOX2 and autophagy proteins. *Nat. Cell Biol.* **17**, 893–906 (2015).
53. M. A. Bewley *et al*., Pneumolysin activates macrophage lysosomal membrane permeabilization and executes apoptosis by distinct mechanisms without membrane pore formation. *MBio* **5**, e01710–e01714 (2014).
54. D. J. Klionsky *et al*., Guidelines for the use and interpretation of assays for monitoring autophagy (3rd edition). *Autophagy* 12, 1–222 (2016).
55. K. Matsunaga *et al*., Two Beclin 1-binding proteins, Atg14L and Rubicon, reciprocally regulate autophagy at different stages. *Nat. Cell Biol.* **11**, 385–396 (2009).
56. C. S. Yang *et al*., The autophagy regulator Rubicon is a feedback inhibitor of CARD9-mediated host innate immunity. *Cell Host Microbe* **11**, 277–289 (2012).
57. S. Y. Kim *et al*., Antibacterial strategies inspired by the oxidative stress and response networks. *J. Microbiol.* **57**, 203–212 (2019).
58. D. Vilchez, I. Saez, A. Dillin, The role of protein clearance mechanisms in organismal ageing and age-related diseases. *Nat. Commun.* **5**, 5659 (2014).
59. N. González-Juarbe *et al*., Pore-forming toxins induce macrophage necroptosis during acute bacterial pneumonia. *PLoS Pathog.* **11**, e1005337 (2015).
60. N. Fujita *et al*., Recruitment of the autophagic machinery to endosomes during infection is mediated by ubiquitin. *J. Cell Biol.* **203**, 115–128 (2013).
61. A. Choy, C. R. Roy, Autophagy and bacterial infection: An evolving arms race. *Trends Microbiol.* **21**, 451–456 (2013).
62. G. Mitchell *et al*., *Listeria monocytogenes* triggers noncanonical autophagy upon phagocytosis, but avoids subsequent growth-restricting xenophagy. *Proc. Natl. Acad. Sci. U.S.A.* **115**, E210–E217 (2018).
63. M. B. Mestre, C. M. Fader, C. Sola, M. I. Colombo, Alpha-hemolysin is required for the activation of the autophagic pathway in Staphylococcus aureus-infected cells. *Autophagy* **6**, 110–125 (2010).
64. N. von Muhlinen, T. Thurston, G. Ryzhakov, S. Bloor, F. Randow, NDP52, a novel autophagy receptor for ubiquitin-decorated cytosolic bacteria. *Autophagy* **6**, 288–289 (2010).
65. I. Nakagawa *et al*., Autophagy defends cells against invading group A Streptococcus. *Science* **306**, 1037–1040 (2004).
66. G. Bensi *et al*., Multi high-throughput approach for highly selective identification of vaccine candidates: Tthe Group A Streptococcus case. *Mol. Cell. Proteomics* **11**, M111.015693 (2012).
67. J. A. Walker, R. L. Allen, P. Falmagne, M. K. Johnson, G. J. Boulnois, Molecular cloning, characterization, and complete nucleotide sequence of the gene for pneumolysin, the sulfhydryl-activated toxin of *Streptococcus pneumoniae*. *Infect. Immun.* **55**, 1184–1189 (1987).
68. K. E. Price, N. G. Greene, A. Camilli, Export requirements of pneumolysin in *Streptococcus pneumoniae*. *J. Bacteriol.* **194**, 3651–3660 (2012).
69. K. M. Davis, H. T. Akinbi, A. J. Standish, J. N. Weiser, Resistance to mucosal lysozyme compensates for the fitness deficit of peptidoglycan modifications by *Streptococcus pneumoniae*. *PLoS Pathog.* **4**, e1000241 (2008).
70. Y. E. Korchev *et al*., A conserved tryptophan in pneumolysin is a determinant of the characteristics of channels formed by pneumolysin in cells and planar lipid bilayers. *Biochem. J.* **329**, 571–577 (1998).
71. M. A. Delgado, V. Deretic, Toll-like receptors in control of immunological autophagy. *Cell Death Differ.* **16**, 976–983 (2009).
72. R. Malley *et al*., Recognition of pneumolysin by Toll-like receptor 4 confers resistance to pneumococcal infection. *Proc. Natl. Acad. Sci. U.S.A.* **100**, 1966–1971 (2003).
73. K. Subramanian *et al*., Pneumolysin binds to the mannose receptor C type 1 (MRC-1) leading to anti-inflammatory responses and enhanced pneumococcal survival. *Nat. Microbiol.* **4**, 62–70 (2019).
74. J. M. Jaynes *et al*., Mannose receptor (CD206) activation in tumor-associated macrophages enhances adaptive and innate antitumor immune responses. *Sci. Transl. Med.* **12**, eaax6337 (2020).
75. C. A. Hinojosa *et al*., Enteric-delivered rapamycin enhances resistance of aged mice to pneumococcal pneumonia through reduced cellular senescence. *Exp. Gerontol.* **47**, 958–965 (2012).
76. D. I. Brown, K. K. Griendling, Nox proteins in signal transduction. *Free Radic. Biol. Med.* **47**, 1239–1253 (2009).
77. A. J. Standish, J. N. Weiser, Human neutrophils kill *Streptococcus pneumoniae* via serine proteases. *J. Immunol.* **183**, 2602–2609 (2009).
78. S. Scharf *et al*., Streptococcus pneumoniae induces human β-defensin-2 and -3 in human lung epithelium. *Exp. Lung Res.* **38**, 100–110 (2012).
79. D. N. Mitzel, V. Lowry, A. C. Shirali, Y. Liu, H. W. Stout-Delgado, Age-enhanced endoplasmic reticulum stress contributes to increased Atg9A inhibition of STING-mediated IFN-β production during Streptococcus pneumoniae infection. *J. Immunol.* **192**, 4273–4283 (2014).
80. J. Lee, S. Giordano, J. Zhang, Autophagy, mitochondria and oxidative stress: Cross-talk and redox signalling. *Biochem. J.* **441**, 523–540 (2012).
81. H. O. Rashid, R. K. Yadav, H. R. Kim, H. J. Chae, ER stress: Autophagy induction, inhibition and selection. *Autophagy* **11**, 1956–1977 (2015).
82. D. Senft, Z. A. Ronai, UPR, autophagy, and mitochondria crosstalk underlies the ER stress response. *Trends Biochem. Sci.* **40**, 141–148 (2015).
83. M. Plataki *et al*., Mitochondrial dysfunction in aged macrophages and lung during primary *Streptococcus pneumoniae* infection is improved with pirfenidone. *Sci. Rep.* **9**, 971 (2019).
84. S. Nakamura *et al*., Suppression of autophagic activity by Rubicon is a signature of aging. *Nat. Commun.* **10**, 847 (2019).
85. T. Yamamuro *et al*., Age-dependent loss of adipose Rubicon promotes metabolic disorders via excess autophagy. *Nat. Commun.* **11**, 4150 (2020).
86. C. P. Verschoor, J. Johnstone, M. Loeb, J. L. Bramson, D. M. Bowdish, Anti-pneumococcal deficits of monocyte-derived macrophages from the advanced-age, frail elderly and related impairments in PI3K-AKT signaling. *Hum. Immunol.* **75**, 1192–1196 (2014).
87. E. Scallan *et al*., Bacterial enteric infections among older adults in the United States: Foodborne diseases active surveillance network, 1996-2012. *Foodborne Pathog. Dis.* **12**, 492–499 (2015).
88. A. Gluschko *et al*., The beta2 integrin Mac-1 induces protective LC3-associated phagocytosis of Listeria monocytogenes. *Cell Host Microbe* **23**, 324–337.e325 (2018).
89. J. M. J. Tan *et al*., An ATG16L1-dependent pathway promotes plasma membrane repair and limits *Listeria monocytogenes* cell-to-cell spread. *Nat. Microbiol.* **3**, 1472–1485 (2018).
90. S. Masud, L. van der Burg, L. Storm, T. K. Prajsnar, A. H. Meijer, Rubicon-dependent Lc3 recruitment to *salmonella*-containing phagosomes is a host defense mechanism triggered independently from major bacterial virulence factors. *Front. Cell. Infect. Microbiol.* **9**, 279 (2019).
91. S. E. Winter *et al*., Gut inflammation provides a respiratory electron acceptor for *Salmonella*. *Nature* **467**, 426–429 (2010).
92. S. Rajagopalan, T. T. Yoshikawa, Tuberculosis in the elderly. *Z. Gerontol. Geriatr.* **33**, 374–380 (2000).
93. N. Sopena *et al*., Community-acquired legionella pneumonia in elderly patients: Characteristics and outcome. *J. Am. Geriatr. Soc.* **55**, 114–119 (2007).
94. P. Abnave *et al*., Screening in planarians identifies MORN2 as a key component in LC3-associated phagocytosis and resistance to bacterial infection. *Cell Host Microbe* **16**, 338–350 (2014).
95. M. I. Cheng, C. Chen, P. Engström, D. A. Portnoy, G. Mitchell, Actin-based motility allows *Listeria monocytogenes* to avoid autophagy in the macrophage cytosol. *Cell. Microbiol.* **20**, e12854 (2018).
96. S. Köster *et al*., *Mycobacterium tuberculosis* is protected from NADPH oxidase and LC3-associated phagocytosis by the LCP protein CpsA. *Proc. Natl. Acad. Sci. U.S.A.* **114**, E8711–E8720 (2017).
97. A. Choy *et al*., The *Legionella* effector RavZ inhibits host autophagy through irreversible Atg8 deconjugation. *Science* **338**, 1072–1076 (2012).
98. K. S. Akagawa *et al*., Functional heterogeneity of colony-stimulating factor-induced human monocyte-derived macrophages. *Respirology* **11** (suppl.), S32–S36 (2006).
99. Y. Kabeya *et al*., LC3, a mammalian homologue of yeast Apg8p, is localized in autophagosome membranes after processing. *EMBO J.* **19**, 5720–5728 (2000).
100. C. L. Birmingham *et al*., *Listeria monocytogenes* evades killing by autophagy during colonization of host cells. *Autophagy* **3**, 442–451 (2007).